

Lower limb models used for biomechanical analysis of human walking

Ludwin Molina^[0000-0002-4171-3483] and Marek Iwaniec^[0000-0002-1224-4753]

Department of Process Control, Faculty of Mechanical Engineering and Robotics, AGH University of Science and Technology, Cracow, Poland

Abstract. Over time, many researchers have focused on creating models to mathematically represent movements performed by human lower limbs, such as walking, running, and jumping. These models provide a non-invasive method to estimate kinematic and kinetic parameters under different conditions. This article reviews the main lower limb models used to study human walking and compares their performance with a 3D model consisting of seven links created using the simulation environment *Simscape Multibody*. A description of each model is presented, highlighting its main characteristics and the assumptions that led to its formulation. We execute numerical simulations based on the first-order Euler method to solve the differential equations resulting from the models' implementation.

1 Introduction

Walking is one of the essential activities that humans perform in their daily lives and, like each of the body movements, involves complex interactions between the neuromuscular and skeletal systems. Understanding these interactions allows not only the design of medical applications [1] for people with movement disabilities but also the development of robotic applications [2]. Many researchers have studied human gait through different methods, such as force platforms [3], digital image recording [4], and motion tracking using fast video cameras or wearable sensors [5, 6].

The modeling of human gait can be formulated from different perspectives. The simplest models use mechanical analogies to study the behavior of global parameters such as the center of mass (COM). In contrast, complex models can be used to study the behavior of a large number of variables considering assumptions that are closer to reality. Various approaches are used to obtain the mathematical expressions that describe the motion of modeled systems. Newton's motion equations represent the most basic tool for understanding the cause-effect relationship of the forces acting on a system and the motion described by it. However, its application to complex systems with a high number of degrees of freedom implies the formulation and resolution of a large number of equations, which results in a high computational cost [7]. The Euler-Lagrange method is widely used in multibody systems since it analyzes the entire system without the need to study the reaction and contact forces that exist between the elements that make up the system [8]. Using the Euler-Lagrange method, we can obtain the equation of motion by dealing only with the

system's mechanical energy. Knowing the equation of motion resulting from the proposed models, the researchers study the mechanics of motion through simulations, identify problems and design mechanisms that seek to imitate, in the case of robots, or recover motion in the case of rehabilitation devices.

The work presented in this article can be divided into two main stages. In the first stage, we review the main lower limb models used for the analysis of the human gait. We present a description of the main characteristics, limitations, and assumptions taken into account during the formulation of each of the reviewed models and the arithmetic and differential equations resulting from their application. In the second stage, we perform gait modeling by creating a 3D model using the simulation environment *Simscape Multibody*. The created model consists of seven rigid segments representing the legs and torso, and rotational joints that connect them. The contribution of this work is to carry out a collection of theoretical knowledge on the modeling of human gait, compare selected models, and present the possibility of modeling human gait in the Matlab Simulink environment.

2 Human walking modeling

To study the behavior of the musculoskeletal system, researchers formulate simplified biomechanical models. These models are often based on classic mechanical systems, such as the inverted pendulum. The use of simplified models allows a general study of gait by examining a reduced number of parameters, facilitating the understanding of cause-effect relationships. Most simplified models reduce the study of complex interactions of the musculoskeletal system to the kinematic study of its COM. This section briefly describes the simplified lower limb models used for the biomechanical study of human walking. The motion equation and the assumptions considered to obtain the mathematical expressions are presented for each model.

2.1 Inverted pendulum

The inverted pendulum model is the simplest model for studying normal gait. This model assumes that the COM follows an arc path above the support leg during the stance phase [9]. The body COM is analogous to the pendulum mass, while the center of pressures on the foot is analogous to the pendulum pivot.

Fig. 1 presents a scheme of the model and the trajectory described by the body COM. The model consists of a bar of negligible weight and length l representing the subject's leg and a point mass M attached to the bar's end analogous to the pedestrian's total mass.

The inverted pendulum model allows predicting a large number of observations made in motion analysis laboratories with a reasonable degree of precision. It has been used to simulate the duration of the spring phase, study the mechanism of gait stability control in the absence of active muscle control, and study COM vertical movements' dependence on leg rigidity during walking.

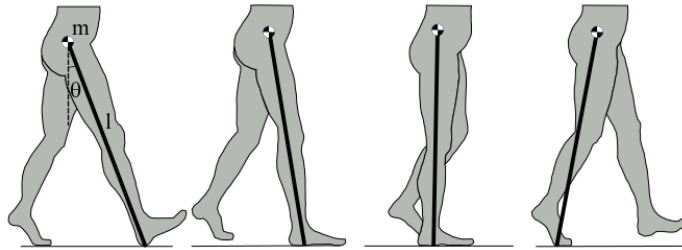


Fig. 1. Inverted pendulum model.

The motion equation for the model is determined by the second-degree nonlinear equation presented below:

$$\ddot{\theta} = \frac{g}{l} \sin \theta \quad (1)$$

where θ and $\ddot{\theta}$ are the angular displacement and acceleration of the pendulum, respectively. g is the gravity acceleration and l is the length of the pendulum representing the length of the lower limb.

Among the limitations of using the inverted pendulum model, there is the inefficiency when using sensors fixed to the body since it is difficult to deduce the acceleration from the COM of the pedestrian. Additionally, a double integration is required to estimate the COM displacement, which results in a rapid propagation of the measurement device's error.

2.2 Passive dynamic walking

McGeer introduced the concept of passive dynamic walking in 1990 [10]. The basic idea behind dynamic passive walking is that the energy lost in inelastic collisions would be compensated by the kinetic energy obtained when the walker descends a ramp. In this way, it is possible to get a stable walk without introducing any external energy supply to the system. The main advantage of this approach is that the obtained expressions only depend on the system's geometric and inertial properties and the ramp's inclination. Several models are derived from the model proposed by McGeer. Most representatives are the compass-like model and the point foot walker model. We present a brief description of the assumptions taken into account in these models and the motion equations resulting from applying the Euler-Lagrange method.

Compass-like biped model

The compass walking model [11] simulates a biped walker's COM trajectory, which descends an inclined plane. The two lower extremities are represented by rigid bars of a point mass m . **Fig. 2** shows a basic outline of the model.

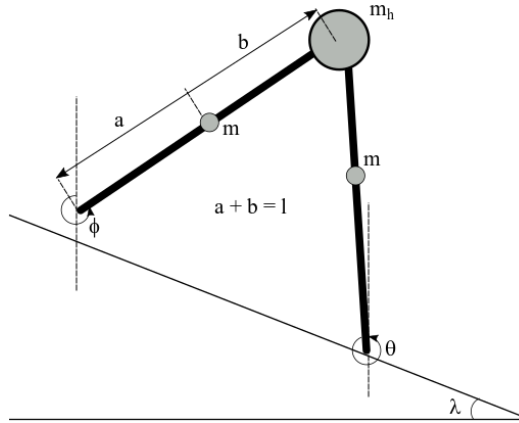


Fig. 2. Compass like biped model.

In this model, each leg has a length l and a point mass m . The hip joint connects the two links and a point mass m_h that represents the weight of the upper body. The stance leg behaves like an inverted pendulum, which is pivoted at the point of contact with the ground, while the spring leg acts like a simple pendulum whose pivot moves. Once the spring leg makes contact with the ground, assuming there are no impulsive forces, a phase transition occurs.

The model's governing equations consist of a series of nonlinear differential equations for the swing and stance phase and algebraic equations for the transition between the stages. The set of differential equations is presented below.

$$M(\theta)\ddot{\theta} + N(\theta, \dot{\theta})\dot{\theta} + g(\theta) = 0 \quad (2)$$

where $M(\theta)$, $N(\theta, \dot{\theta})$ and $g(\theta)$ are symmetric matrices whose values are given by the expressions presented below and depend on the system's inertial and geometric parameters.

$$M(\theta) = \begin{pmatrix} mb^2 & -mlb \cos(\theta - \phi) \\ -mlb \cos(\theta - \phi) & m_h l^2 + m(l^2 + a^2) \end{pmatrix} \quad (3)$$

$$N(\theta, \dot{\theta}) = \begin{pmatrix} 0 & -mlb \dot{\theta} \sin(\theta - \phi) \\ -mlb \dot{\phi} \sin(\theta - \phi) & 0 \end{pmatrix} \quad (4)$$

$$g(\theta) = \begin{pmatrix} mgb \sin \phi \\ -(m_h l + m(a + l))g \sin \theta \end{pmatrix} \quad (5)$$

where m is the mass of each leg. a is the length measured from the bottom end to the COM. b is the length to the COM measured from the top end. l is the length of the leg. θ , $\dot{\theta}$, and $\ddot{\theta}$ are the angular position, velocity, and acceleration of the stance leg, respectively. ϕ , $\dot{\phi}$, and $\ddot{\phi}$ are the angular position, velocity, and acceleration of the spring leg, respectively. m_h is the total mass of the body and g is the gravity acceleration.

The algebraic equation for modeling the transition between phase is obtained from formulating the conservation of the angular momentum at the heelstrike. For information about this calculation, the reader can refer to [12].

Point foot walker

The point foot walker[13], also known as the simplest walking model, is a derivation of the compass gait model, and it was proposed by Garcia et al. in 1997. The schematic representation of the model is shown in Fig. 3. Two links and three mass points make up the model. The links, which represent the human legs, are connected by a frictionless hinge at the hip. The masses are located at the hip joint and the feet. The mass M located at the hip joint represents the mass of the upper body, which is much larger than the foot mass m so that the motion of a stance leg does not affect the swing leg's movement. Additionally, the mechanism moves on a ramp with slope λ .

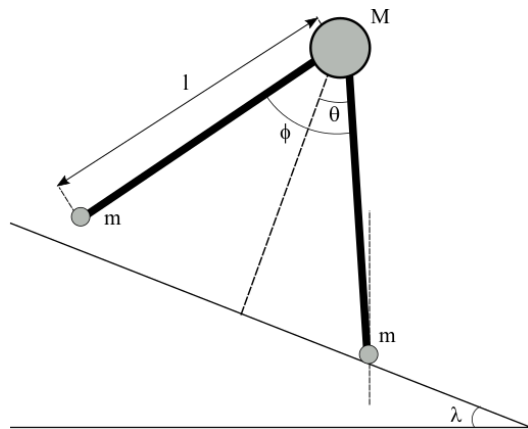


Fig. 3. Point foot walker model (the simplest walking model).

The laws of classical rigid-body mechanisms govern the model's motion. Through the Lagrange equations, it is possible to get the expressions of movement of the system. To reduce the model's complexity, the author assumes that the mass point M is much greater than the mass points m . For this reason, the mass terms are not found on the equations.

$$\ddot{\theta} = \frac{g}{l} \sin(\theta - \phi) \tag{6}$$

$$\ddot{\phi} = \ddot{\theta} + \dot{\theta}^2 \sin \phi - \frac{g}{l} \cos(\theta - \phi) \sin \phi \tag{7}$$

where θ , $\dot{\theta}$ and $\ddot{\theta}$ are the angular position, velocity, and acceleration of the stance leg, respectively. ϕ , $\dot{\phi}$, and $\ddot{\phi}$ are the angular position, velocity, and acceleration of the spring leg, respectively. l is the length of the leg and g the gravity acceleration.

Equation(6) represents the movement of an inverted pendulum without the influence of the swing leg's motion. In contrast, Equation (7) describes the behavior of a simple pendulum whose support moves through an arc path.

Besides the differential equations that describe the motion of the spring and stance leg, it is necessary to impose a transition rule when the swing foot hits the ground at heelstrike. The collision occurs when the following geometric condition occurs.

$$\phi - 2\theta = 0 \tag{8}$$

At heelstrike, there is an impulse at the swing foot contact point. We assume the new stance leg has no impulsive reaction to the ground. Therefore, the angular momentum is conserved at the collision for the whole mechanism around the swing foot contact point and the new stance leg around the hip joint. From the angular momentum conservation, we get the transition rules presented in (9), where the + subscripts mean just after the collision and the – just before the collision.

$$\begin{bmatrix} \theta \\ \dot{\theta} \\ \phi \\ \dot{\phi} \end{bmatrix}^+ = \begin{pmatrix} -1 & 0 & 0 & 0 \\ 0 & \cos 2\theta & 0 & 0 \\ -2 & 0 & 0 & 0 \\ 0 & \cos 2\theta(1 - \cos 2\theta) & 0 & 0 \end{pmatrix} \begin{bmatrix} \theta \\ \dot{\theta} \\ \phi \\ \dot{\phi} \end{bmatrix}^- \tag{9}$$

2.3 Ballistic walking

Based on a compass gait mechanical model, ballistic models refer to analyzing the swing phase of the gait cycle[14]. Mochon and McMahon showed that the body's forward movement during the swing phase could be accomplished in the absence of any muscle force generation and only from a set of kinematic conditions and constraints, i.e., setting the swinging leg velocity at the instance of toe lift. The human body's behavior during the oscillation phase is due to the influence of gravity and imposed restrictions on the conservation of mechanical energy. A set of kinematic conditions is set up at the initial contact for the continuity of the motion. The leg performs similarly to that of a simple pendulum assuming no muscular activities during this phase.

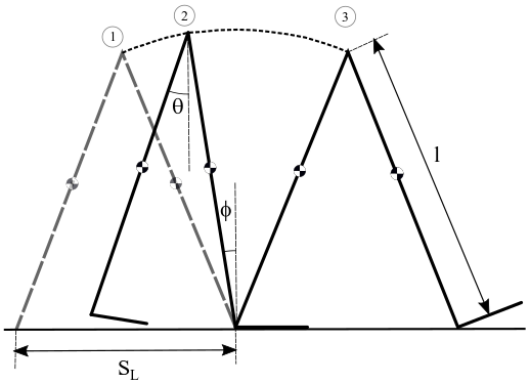


Fig. 4. Schematic representation of the ballistic model.

Fig. 4 shows a schematic representation of the model. The numbers 1, 2, and 3 give, respectively, the position of the model at heelstrike, toe-off, and the following heelstrike. This model consists of two links representing each leg. We assume each link is a rigid body with distributed mass, and a mass point represents the mass of the trunk head and arms at the hip joint. Based on this model, two approaches can be considered: one assumes stiff-legged walking, and the other takes into account the knee's flexion. In this paper, we only present stiff-legged walking. For information about the model considering flexion knee, the reader can

refer [14]. The dynamic equations resulting from applying the Euler-Lagrange method on the stiff-legged walking model are presented below:

$$\begin{aligned} J\ddot{\theta} - C\dot{\phi}^2 \sin(\theta - \phi) - C\ddot{\phi} \cos(\theta - \phi) &= U \sin \theta \\ I\ddot{\theta} + C\dot{\theta}^2 \sin(\theta - \phi) - C\ddot{\theta} \cos(\theta - \phi) &= -W \sin \phi \end{aligned} \quad (10)$$

where θ , $\dot{\theta}$ and $\ddot{\theta}$ are the angular position, velocity, and acceleration of the swing leg, respectively. ϕ , $\dot{\phi}$, and $\ddot{\phi}$ are the angular position, velocity, and acceleration of the stance leg respectively. I and m are the moment of inertia and mass of each leg, respectively. M is the mass of the entire body. \bar{Z} is the COMposition of the leg measured vertically. The value of the other constants depends on the below expressions:

$$\begin{aligned} J &= I + Ml^2 - 2m\bar{l}\bar{Z} \\ C &= m\bar{l}\bar{Z} \\ U &= (Ml - m\bar{l}\bar{Z})g \\ W &= m\bar{Z}g \end{aligned}$$

Below, we present the kinematic conditions and limitations that must be met to guarantee the mechanism's motion continuity.

$$\begin{aligned} \theta(0) &= -\phi(0) \\ \theta(T_s) &= -\phi(T_s) \\ S_L(0) &= S_L(T_s) \end{aligned} \quad (11)$$

where T_s is the duration time of a step and S_L the step length.

Additionally, the author emphasizes the need for fulfilling two additional dynamic constraint. The first constraint is that the ground's vertical reaction force must always be positive; otherwise, it means the body is flying. The second constraint is that the swing leg's initial angular velocity should be positive because if it is negative, the leg will swing backward at the beginning of the swing phase. Although these constraints are not being mentioned before, they are necessary conditions for all the models mentioned in this report.

2.4 Active dynamic walking

Active dynamic walking models consist of a series of rigid elements connected by joints and actuated by controlled torques. This type of model pursues tracking joint angles throughout the gait cycle by supplying mechanical power to drive the joints [15].

To the construction of an active dynamic model, the researchers require anthropometric data. The model's precision depends on how accurate the data used for constructing the rigid elements that make up the model is. One of the advantages of this kind of model is the possibility of representing both gait phases; spring and stance phase. As in the passive dynamic models, we obtain the motion equation by using the LaGrange approach. Some assumptions are generally considered, such as a homogeneous mass distribution and the neglect of friction over the joints. The resulting motion equation is a matrix representation similar to the obtained from the models presented above, whose grade of freedom depends on the number of elements that make up the mechanism.

$$M(\theta)\ddot{\theta} + C(\theta, \dot{\theta})\dot{\theta} + G(\theta) = \tau \quad (12)$$

Where $M(\theta, \dot{\theta})$ is the inertial matrix. $C(\theta, \dot{\theta})$ is the Coriolis matrix. $G(\theta)$ is the gravitational matrix, and τ the driver moment around the joint.

An essential point in the formulation of the active lower limb model is the correct representation of the contact between the foot and the ground. There are several approaches to lead with the impact phenomenon. One of the most used strategies is treating the ground as a solid infinitive body with a stiffness and damping coefficient [16]. Mathematically the contact force is calculated through the following expression:

$$F_c = k\delta + c\dot{\delta} \tag{13}$$

Where δ , $\dot{\delta}$ are the deformation and rate deformation produced by the sole-ground contact. k and c are the stiffness and damping coefficient, respectively.

3 Simulation

Based on the models presented above, we perform numerical simulations to solve the differential equations associated with the lower limb motion in each of the different cases. For this study, we selected three of the presented models; the inverted pendulum, the point foot walker model, and a 3D model of seven links created through the software tool *Simscape Multibody*.

3.1 Parameters for the simulation

Inverted pendulum:

Table 1. Parameters for the inverted pendulum.

Parameter	Description	Value
l	Leg longitude	$0.9\ m$
M	Mass point at the hip	$80\ kg$

Point foot walker:

Table 2. Parameters for the point foot walker model.

Parameter	Description	Value
l	Leg longitude	$0.9\ m$
M	Mass point at the hip	$80\ kg$
λ	Slope angle	$0.00015\ rad$

Active model:

The created model consists of seven rigid links whose dimensions were adjusted based on the anthropometric data taken from [17]. Three links make up each leg, representing the shank, leg, and foot. The last link plays the role of the upper body. Additionally, we create a plane with considerable length to serve as the floor.

The model was elaborated using the tool MathWorks product *Simscape multibody*. This tool allows the connection of mechanical elements and simulates the system's behavior under different boundary conditions through a graphical environment. The connections

between the links are hinge-type connections, allowing only one rotational motion. In the same way, we constraint the upper body to be incapable of rotating to appreciate the COM displacement just under the lower limb movements' influence. Fig. 5 shows the block diagram of the constructed model. Ground-foot contact is modeled by adding a restoring force below the foot surface depending on selected stiffness and damping parameters. We set up a stiffness and damping coefficient for the floor plane and treat the sole as four perfect spheres. Therefore, the foot-ground contact's reaction force depends on the overlapping between the floor plane and the four spheres making the foot. A screenshot of the graphical interface of the constructed model is depicted in Fig. 6.

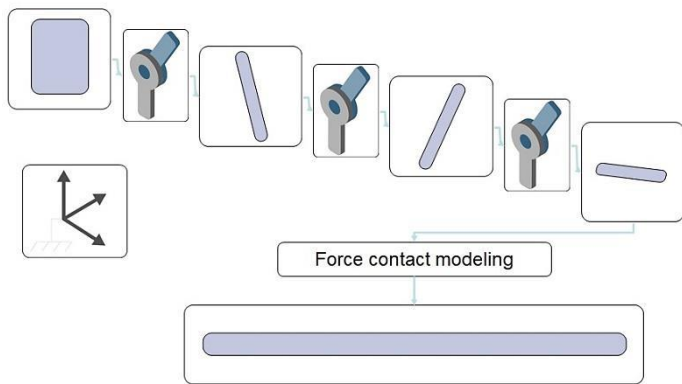


Fig. 5. Block diagram of the created3D seven-links model.

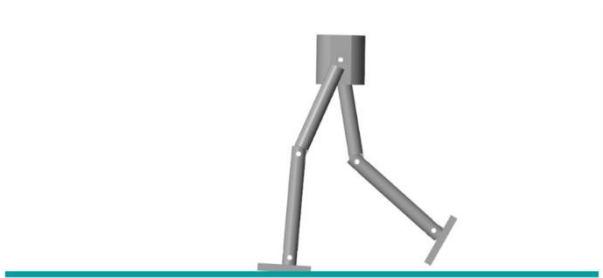


Fig. 6. 3D seven-links model created using Simscape multibody.

The complete data used for the model elaboration is presented in Table 3. The input data for the motion of each joint was taken from the research carried out in [18].

Table 3. Parameters for the creation of the 3D seven-links lower limb model.

Parameter	Description	Value
m_1	Mass of the shank	4.889 <i>kg</i>
m_2	Mass of the thigh	5.664 <i>kg</i>
m_3	Mass of foot	1.5 <i>kg</i>
l_1	Length of shank	0.419 <i>m</i>
l_2	Length of thigh	0.421 <i>m</i>
l_3	Length of foot	0.225 <i>m</i>
I_1	Moment of inertia of shank	0.04202 <i>kg · m²</i>
I_2	Moment of inertia of thigh	0.0982 <i>kg · m²</i>
I_3	Moment of inertia of the foot	0.01005 <i>kg · m²</i>

3.2 Simulation Methods

The resulting differential equations from the formulation of the presented models were solved using Euler's method. Euler's method is a first-order numerical procedure used to solve ordinary differential equations with a given initial condition [19]. The basis of this method is to replace the differentiation, which is a continuous process, by finite differences (discrete process).

Considering the form of the ordinary differential equation:

$$\frac{dy}{dt} = f(t,y)$$

(14)

We used the Taylor series expansion truncated at the first term to obtain a first-order approximation of the solution for the given differential equation presented in (14).

$$y_{i+1} = y_i + f(t,y)(t_{i+1} - t_i)$$

(15)

where the *i* is the number of the evaluated sample and *t_{i+1} - t_i* is the length of the step between two evaluated samples.

4 Results and Discussion

The results obtained from the inverted pendulum, point foot walker, and 3D seven link model are presented below. Since the support leg in the case of the point foot walker model behaves exactly like an inverted pendulum, we decided not to show result figures for both models. To appreciate the inverted pendulum model results, the reader should refer only to the support leg results showed in the figures of the point foot walker model. Fig. 7 shows from top to bottom the angular displacement, velocity, and acceleration of the links, which make up the point foot walker model. The blue line shows the angular motion of the stance leg (inverted pendulum), while the orange line presents the motion of the swing leg. We can observe that the pendulum starts from a positive position concerning the reference, which is the fully vertical position. The angle of the pendulum decreases until it

reaches its corresponding initial value with an inverted sign. For this movement to take place, it is crucial to adjust the initial speed of the pendulum since otherwise, the pendulum would fall due to the effect of gravity.

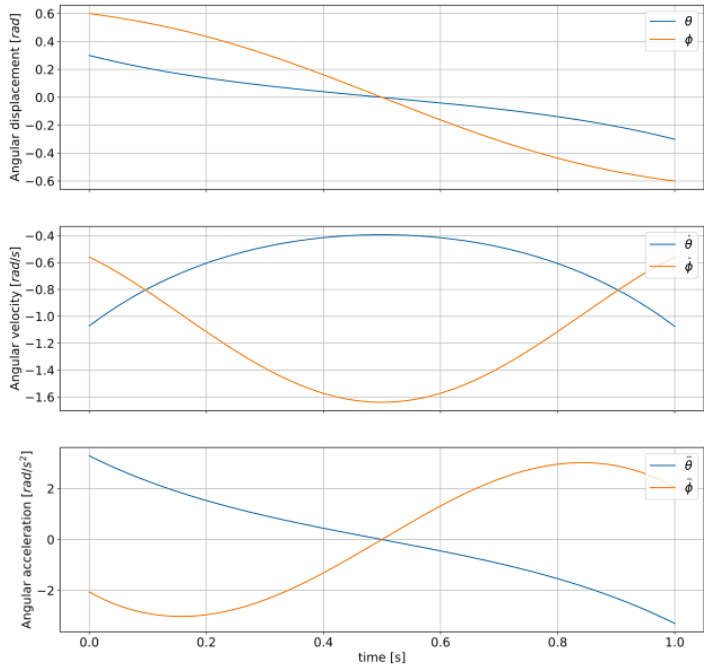


Fig. 7. Angular position, velocity, and acceleration of the point foot walker model.

Fig. 8 presents the COM motion of the inverted pendulum and point foot walker model, which, as predicted, is a semi-circular movement. The blue line represents the support leg that has the same behavior of the inverted pendulum since the model considers the mass of the feet so minimal that it does not affect the global movement. Besides an adequate initial velocity, we imposed the fulfillment of the transition condition presented in (9), which gives us a cyclical repetition of the graphs presented in Fig. 7 and Fig. 8 if we extend the simulation time.

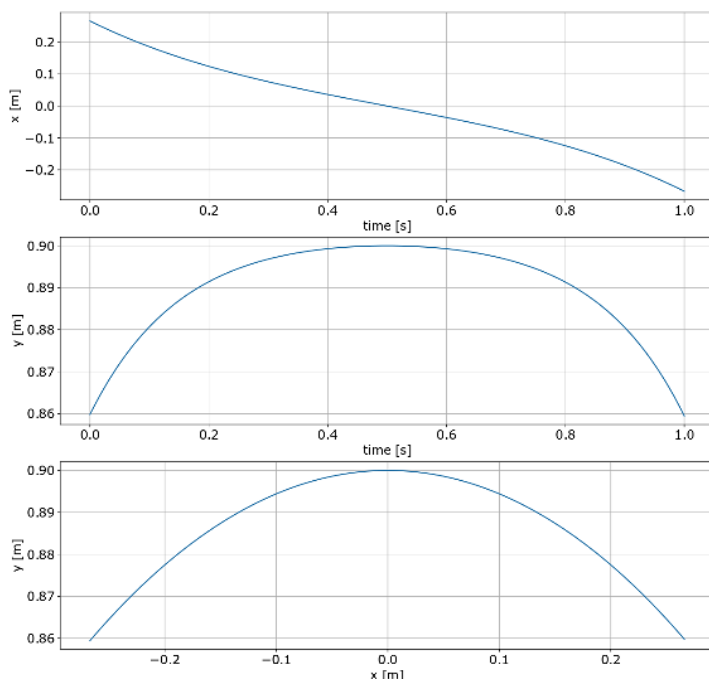


Fig. 8. Motion described by the COM (point-foot walker model).

By applying the fundamental equations of mechanics, we obtained the reaction forces in the horizontal and vertical direction. These forces in the model are analogous to the foot-ground contact force and friction force. The results of this procedure are presented in Fig. 9, where the red line shows the variation of the tangential foot-ground contact force, and the blue line presents the behavior of the normal contact force.

We can appreciate that the normal contact force is minimal when the pendulum is in a vertical position, due to the absence of inertial forces. On the other hand, the friction force changes sign as the pendulum moves between left and right.

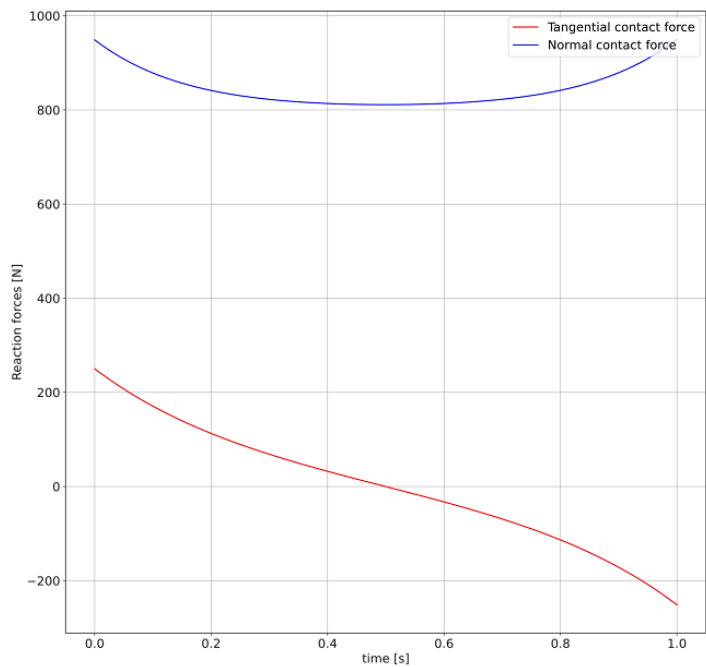


Fig. 9. Reaction forces produced along the gait cycle obtained from the point foot walker model.

Fig. 10 presents the COM motion for the designed 3D seven-links model. To compare the point foot walker model, the reader must limit the results to the same time of simulation presented in the results of the point walker model. *Simscape multibody* tool also allow to determine the driving torques that make possible to get the targeted movements of for lower limb joints, as well as the reaction forces resulting by the ground-foot contact. The vertical ground-foot contact reaction force and the joints driving torques are depicted in Fig. 11. Based on the results obtained through the numerical simulations performed for the inverted pendulum, pointed walker, and the 3D seven-links model, we can see that the path followed by the COM is indeed an arc for all the models. In the case of the inverted pendulum and the point-foot walker, the arc described by the COM has slow growth compared to the arc described by the 3D seven-link model. Regarding the kinetic parameters, the 3D seven-links model provides additional information since it considers the three major joints that make up the lower limb. The vertical ground reaction forces calculated for the three models globally show similar behavior. In the case of the inverted pendulum and foot-point walker models, we observe a curve with a local minimum in the center, while in the case of the 3D seven-linksmodel, each gait cycle has two local maximums and one local minimum also located at the center. The behavior described by the inverted pendulum is an easy mathematical approximation to implement, however, it does not reflect important details that are required from gait analysis. On the other hand, the behavior of the 3D seven-links model is more realistic.

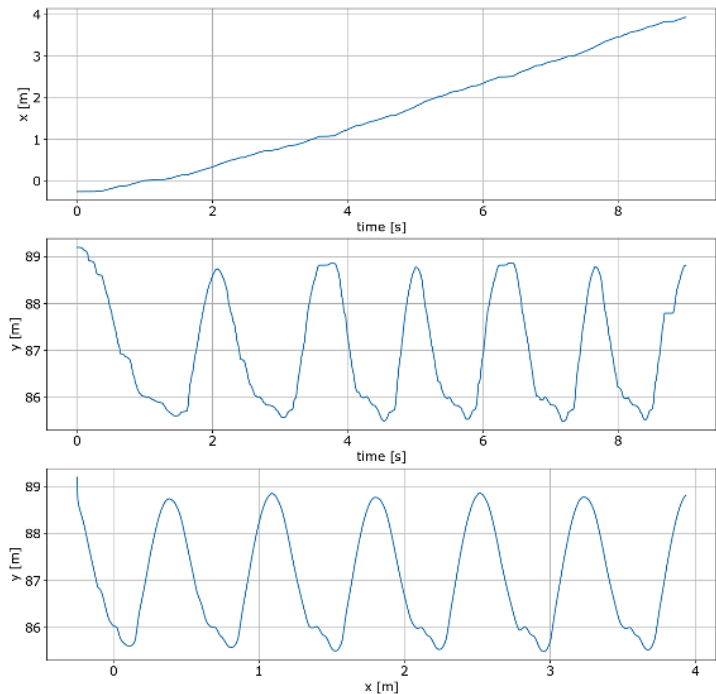


Fig. 10. Motion described by the COM obtained from the 3D seven-links model.

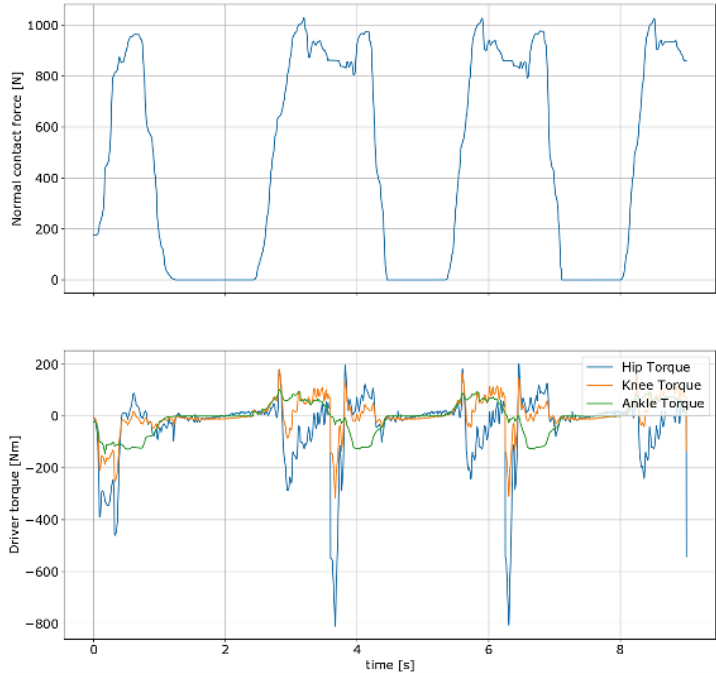


Fig. 11. Ground-foot vertical reaction force and driving torques over the joints obtained from the 3D seven-links model.

5 Conclusions

In this study, we presented simplified lower limb models used for the biomechanical analysis of human walking. These models are an idealized mathematical approach to the study of human gait and provide a preliminary understanding of his fundamental concepts. We did not consider the effect of muscles and the nervous system on the model elaboration since the neurological control of the gait is still under study, and there is not complete certainty about how the algorithm of control is used by the brain to control walking.

The differential equations governing motion were determined using the principles of classical mechanics, taking into account the main characteristic of each model as well as the assumption established by his respective author. By using anthropometric data collected from performed research, we ran numerical simulations to estimate kinematic and kinetic variables from the point foot walker and a the designed 3D seven-links model. The obtained results from the simulations evidence a similar behavior of the models regardless of the COM trajectory and foot-ground contact reactions. The simplified models offer a great alternative when the researchers are concern about global kinematic and kinetic parameters—in contrast, increasing the model complexity permit to get a significant quality on the results at a higher computational cost.

References

1. J. Kopowski, I. Rojek, D. Mikołajewski, M. Macko 3D Printed Hand Exoskeleton - Own Concept. In: *Advances in Manufacturing II. Vol. 1 - Solutions for Industry 4.0* / eds. Justyna Trojanowska, Olaf Cizak, José Mendes Machado, Ivan Pavlenko. Springer, Cham, pp 298–306 (2019).
2. A. Omer, H. Kenji, H. Lim, A. Takanashi Study of Bipedal Robot Walking Motion in Low Gravity: Investigation and Analysis. *Int J Adv Robot Syst* (2014).
3. T. Maeda, T. Ishizuka S. Yamaji, Y. Ohgi A Force Platform Free Gait Analysis. *Proceedings*, 2, 207 (2018).
4. J.M.R.S. Tavares, R.M. Natal Jorge Image processing and analysis in biomechanics. *EURASIP J Adv Signal Process* (2010).
5. X. Jiang, M. Gholami, M. Khoshnam, et al. Estimation of ankle joint power during walking using two inertial sensors. *Sensors (Switzerland)* 19, 1–11 (2019).
6. W. Tao, T. Liu, R. Zheng, H. Feng Gait analysis using wearable sensors. *Sensors* 12, 2255–2283 (2012).
7. Ph.D.E. Arus, E Arus *The Fundamentals of Biomechanics*, 2nd ed. Springer (2018).
8. M.W. Spong, S. Hutchinson, M. Vidyasagar *Robot dynamics and control*, 1st ed. John Wiley & Sons (1989)
9. A.D. Kuo The six determinants of gait and the inverted pendulum analogy: A dynamic walking perspective. *Hum Mov Sci*, 26, 617–656 (2007).
10. T. Mcgeer Passive Dynamic Walking. *Int J Rob Res*, 9, 62–82 (1999).
11. A. Goswami, B. Thuilot, B. Espiau A study of the passive gait of a compass-like biped robot: Symmetry and chaos. *Int J Rob Res*, 17, 1282–1301 (1998).
12. A. Goswami, B. Thuilot, B. Espiau B Compass-Like Biped Robot Part I : Stability and Bifurcation of Passive Gaits. *Res Report*] 2996–73701 (1996).
13. M. Garcia, A. Chatterjee, A. Ruina, M. Coleman The Simplest Walking Model: Stability, Complexity, and Scaling. *J Biomech Eng* 120, 281–288, 1998.
14. S. Mochon, T.A. McMahon Ballistic walking. *J Biomech* 52:241–260, (1980).

15. S.M. Nacy, S.S. Hassan A Modified Dynamic Model of the Human Lower Limb During Complete Gait Cycle. *Int J od Mech Eng Robot Res* 2, 12 (2013).
16. M.S. Shourijeh, J. McPhee Foot-ground contact modeling within human gait simulations: from Kelvin-Voigt to hyper-volumetric models. *Multibody Syst Dyn* 35:393–407 (2015).
17. K. Cerny Williams and Lissner: *Biomechanics of Human Motion* (1978).
18. G. Bovi, M. Rabuffetti, P. Mazzoleni, M. Ferrarin A multiple-task gait analysis approach: Kinematic, kinetic and EMG reference data for healthy young and adult subjects. *Gait Posture* 33, 6–13 (2011).
19. D.F. Griffiths, D.J. Higham S. Undergraduate, M. Series Euler's Method BT - Numerical Methods for Ordinary Differential Equations: Initial Value Problems. In: Griffiths DF, Higham DJ (eds) *Numerical Methods for Ordinary Differential Equations*. Springer London, London, pp 19–31 (2010).